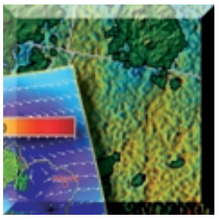

Wind Fields from SAR: Could They Improve Our Understanding of Storm Dynamics?

Kristina B. Katsaros, Paris W. Vachon, Peter G. Black, Peter P. Dodge, and Eric W. Uhlhorn

Four hurricane images obtained by Radarsat were examined. Strong variations in backscatter from the surface in and around convective cells associated with rain cells and rain bands were observed, coupled with increased backscatter in regions of high wind outflow. Long linear features of 3 to 6 km were also noted in three of the four hurricanes, probably due to secondary circulations in the atmospheric boundary layer (roll vortices). They occurred between convective rain bands, where the descending motion could produce a well-defined boundary layer. Although the origins and mechanisms producing the features are still not clear, the high-resolution wide swath coverage modes of synthetic aperture radar provide new insights and present important questions for further research. (Keywords: Hurricanes, Roll vortices, SAR winds, Surface features.)

INTRODUCTION

Synthetic aperture radars (SARs) are regularly flown on satellites, e.g., European Remote Sensing (ERS), Japanese Environmental Resources Satellite, and Radarsat, and several more are in the planning stages. Radarsat can be operated in several modes with wide enough swaths to make the data interesting for storm research.[1] Our goal is to determine what we can learn about tropical storms from SAR data.

During the 1998 hurricane season, four Radarsat images were captured, one each from hurricanes Bonnie, Danielle, Georges, and Mitch. Table 1 shows the hurricane dates and times, and the radar modes and their associated swath widths used to study them. Two swath widths were used. For ScanSAR wide B, the resolution is 100 m, with a swath of about 450 km; for wide 1, the resolution is about 30 m with a swath of about 180 km. All four images were obtained during descending passes.

Radarsat operates in C band and therefore penetrates most rain without much attenuation, but not the intense convection of a hurricane. It is operated in horizontal polarization for both transmit and receive. The ScanSAR modes are not well calibrated, and all Radarsat modes have occasional problems with analog-to-digital converter saturation. Conversion of the backscatter strength to wind speed is a challenge[2] and was not attempted for the discussion here. The four hurricane images show many intriguing features for which we offer some interpretations based on previous work and available supporting measurements from other platforms.

Table 1. Radarsat SAR hurricane images from 1998.

Hurricane	Date/time (UT)	Mode	Scale (km)
Bonnie	27 Aug/1107	ScanSAR wide B	457 × 943
Danielle	31 Aug/1048	ScanSAR wide B	430 × 900
Georges	26 Sep/1135	Wide 1	182 × 330
Mitch	27 Sep/1133	Wide 1	184 × 322

Note: All passes are descending.

BACKGROUND

The SAR returns depend on the roughness of the sea surface. To the extent that the returns depend on the surface wind stress, one can interpret the backscatter in terms of the corresponding wind speed at a particular height. Calibration of the SAR in terms of wind speed is, however, dependent on the calibration of the radar itself, control of the image processing, and knowledge of the wind direction from ancillary sources. In the case of a tropical cyclone, the overall circulation pattern is, of course, known, which makes it useful for calibrating SAR wind algorithms (e.g., Ref. 2). Radar return is affected by other features as well, such as raindrops impinging on the ocean surface and generating roughness that dampens the wind-generated capillary waves and attenuation by rain along the propagation path through the atmosphere. The Radarsat SAR operates at C band (5.6 GHz or 5.6 cm), which is relatively insensitive to normal rainfall but not to the heavy rain of a hurricane.

The 180- or 450-km width of Radarsat images allows a reasonably large portion of a hurricane to be viewed at once, but a random sampling would seldom catch a storm, and regular sampling would have many misses due to the rarity of hurricanes. Thus, obtaining Radarsat wind fields in hurricanes during the Atlantic hurricane season requires some level of serendipity or the opportunity for immediate decision making.

Combining the Radarsat images with other information is essential for interpretation. However, because of the nature of these extreme events and the success of modern warning systems, ships alter their course to avoid storms, and many buoy wind sensors lose power or are simply destroyed before yielding significant high wind data. For interpretation, we rely on the following data sources for our cases:

- Research and reconnaissance aircraft missions by the Hurricane Research Division (HRD) of the Atlantic Oceanographic and Meteorological Laboratory provided airborne scatterometer and radiometer data and flight-level wind data (at about 1600 m). During the 1998 hurricane season, HRD operated Global Positioning System (GPS) dropsondes,[3] which provided wind profiles down to the sea surface from which surface wind fields could be validated.[4]
- For Bonnie and Georges, observed near landfall by Radarsat, we had coverage by the WSR-88D ground-based radars from Morehead City, North Carolina, and Key West, Florida, respectively. They revealed the location of rain bands and rain cells and, in the Doppler mode, gave values for the radial wind speed at the scan level (of the order of 1 km). These next-generation radars (NEXRAD) operate in continuous precipitation mode during hurricane passage, and therefore provide "base scan" images every 6 min, coincident in time to within a few minutes of the SAR images.
- We have also employed visible and infrared satellite observations by the National Oceanic and Atmospheric Administration (NOAA) Geostationary Orbiting Environmental Satellite, the Advanced Very High Resolution Radiometer (AVHRR) polar-orbiting NOAA satellite for sea surface temperature, rain and cloud information from the Special Sensor Microwave Imager (SSM/I) on Defense Meteorological Satellite Program polar-orbiting satellites, and the radar and microwave radiometer on the Tropical Rainfall Measuring Mission (TRMM).

RESULTS

In the following sections, we illustrate the usefulness of SAR images in diagnosing mesoscale structures in each of the four hurricanes as revealed by this new tool for hurricane study.

Bonnie

Figure 1a shows a portion of a SAR image matched in scale with an almost coincident NEXRAD image. We see three distinct features of Bonnie's surface layer: (1) the dark bands characteristic of the leading edge of two segments of a mainly stratiform outer rain band indicated by A and B and referred to[5] as the hurricane "principal rain band"; (2) the alternating dark and bright patches representing the convective nature of the outer band (from C to C′) referred to as the "pre-hurricane squall line"; and (3) banded structures seen mainly southwest of the stratiform principal band and the outer convective band.

The image shows that the stratiform bands A and B lie primarily over the cooler shelf water (26.5–28.5°C) inshore from the north wall of the Gulf Stream as derived from an AVHRR image from JHU/APL (not shown). The outer convective band, C–C′, lies primarily over the Gulf Stream seaward of the north wall and,

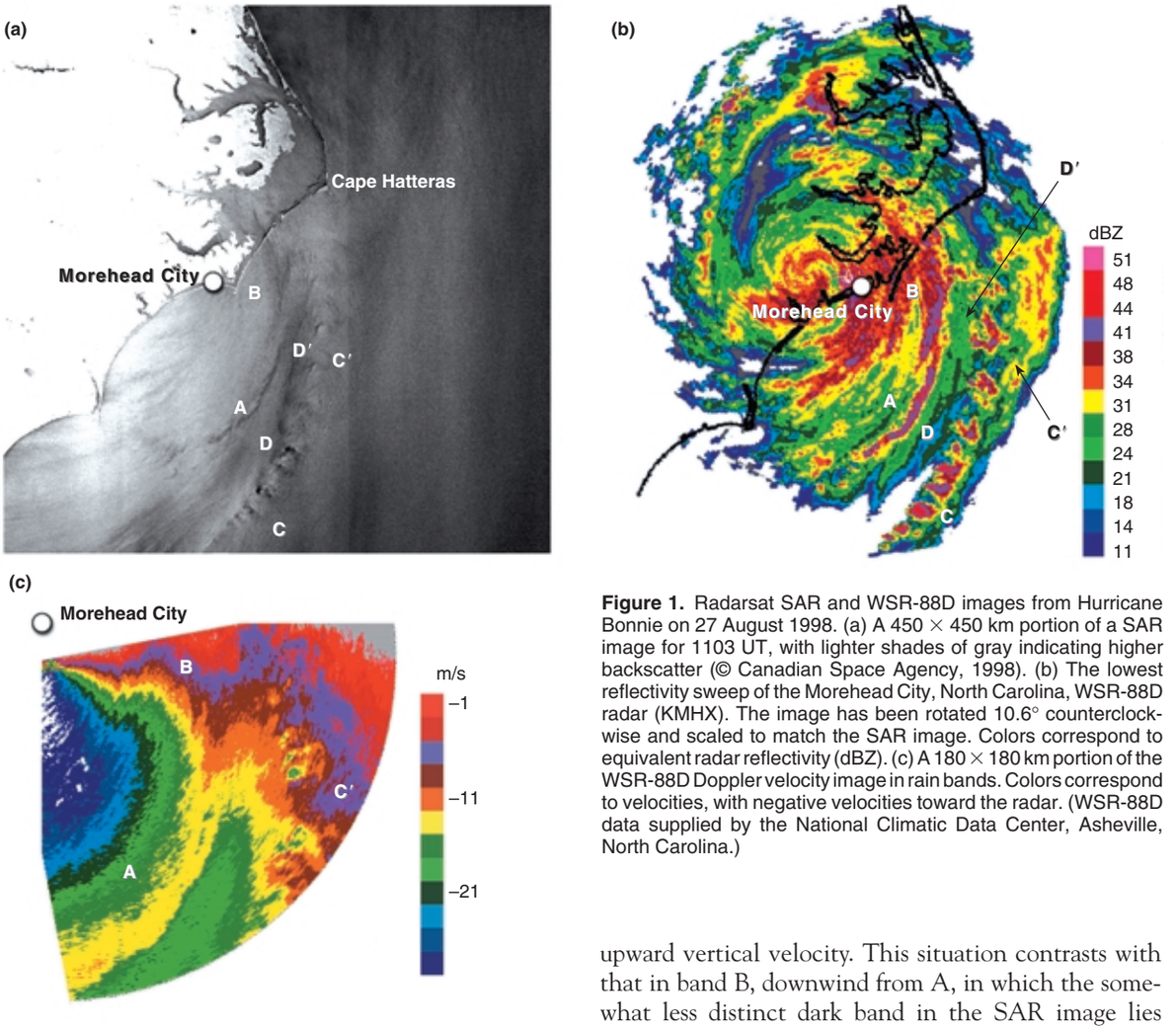

Figure 1. Radarsat SAR and WSR-88D images from Hurricane Bonnie on 27 August 1998. (a) A 450 × 450 km portion of a SAR image for 1103 UT, with lighter shades of gray indicating higher backscatter (© Canadian Space Agency, 1998). (b) The lowest reflectivity sweep of the Morehead City, North Carolina, WSR-88D radar (KMHX). The image has been rotated 10.6° counterclockwise and scaled to match the SAR image. Colors correspond to equivalent radar reflectivity (dBZ). (c) A 180 × 180 km portion of the WSR-88D Doppler velocity image in rain bands. Colors correspond to velocities, with negative velocities toward the radar. (WSR-88D data supplied by the National Climatic Data Center, Asheville, North Carolina.)

hence, over the warm (30–31°C) water near the axis of the Gulf Stream, a factor contributing to the convective nature of the band due to enhanced surface fluxes.

The dark line associated with A seems to be located at the leading edge of the principal rain band. This band is most likely due to a combination of effects: damping of surface capillary waves by heavy raindrop impact, a decrease in the horizontal component of the surface wind at the leading edge of the band where updrafts into the band might be a maximum,[6] and some attenuation of the signal by the intense rain in the atmosphere (for C-band radar, the last effect is less important; personal communication, J. R. Carswell, University of Massachusetts, Amherst, 1999).

The Doppler velocities from the NEXRAD radar (Fig. 1c) measured a dramatic decrease in radial flow across the outer edge of band A of more than 5 m/s over 2 km, indicating strong convergence and associated upward vertical velocity. This situation contrasts with that in band B, downwind from A, in which the somewhat less distinct dark band in the SAR image lies along the middle of the stratiform rain band. In this case, the dark SAR band is probably exclusively a result of the rain damping the capillary waves.

In the outer convective band, C–C′ (Fig. 1b), very high radar reflectivities in excess of 45 dBZ are located somewhat upwind from the dark spots along the band, straddling the region between the dark and adjacent white patches (dBZ = 10 $\log_{10}(z)$, where z is the radar reflectivity factor used in relating received power to the precipitation content of the pulse volume). The white patches appear to be regions of increased surface winds within the convective band, probably a result of strong downdrafts enhancing the existing horizontal winds in the hurricane circulation. Sharp changes in Doppler velocity are also evident in the convective cells at C′ in Fig. 1b.

Another dark band (D–D′ in Fig. 1a) is seen between the outer convective and principal stratiform bands. Radar images from the previous hour showed an additional band between the two major outer bands discussed previously. This band had dissipated by the

time of the SAR overpass. However, it appears that the signature from this rain band had persisted as a coherent dark surface feature for the ensuing 0.5 to 1.0 h. This "hysteresis" effect was noted in the SAR images analyzed by Atlas and Black[7] for thunderstorm cells in a quiescent background wind field.

The next features of interest are seen just southwest of the outer convective band in a sector of the SAR image presented at full resolution in Fig. 2, lower right corner. The wavelength of the linear structures ranges from 3.0 km over the Gulf Stream to 5.5 km in the stronger winds over the shelf water shoreward of the Gulf Stream north wall. These features represent a new scale of boundary-layer secondary circulations not previously identified in hurricanes.

Signatures of convective and roll circulations in the atmospheric boundary layer have been previously documented for Seasat SAR[8] and the ERS-1 SAR[9] in the North Sea. In the latter case, the reported aspect ratio of the observed rolls was 1.65:1 to 3:1. GPS dropsondes deployed in this same region relative to the center of Bonnie on the previous day showed mixed-layer depths on the order of 1 km, with boundary-layer winds of 20 to 25 m/s. If the "roll" circulation was confined to the boundary layer, this would represent an aspect ratio of 3:1 over the Gulf Stream region.

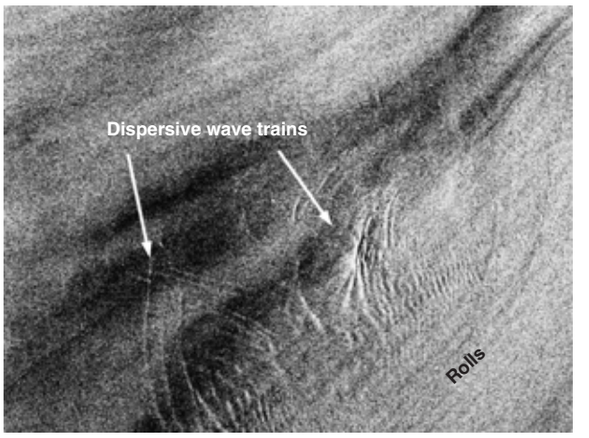

Figure 2. A 128 × 92 km portion of a Radarsat SAR image of Hurricane Bonnie, enhanced to show features with several different wavelengths (© Canadian Space Agency, 1998).

Also seen in Fig. 2 are two dispersive wave trains in the ocean with semicircular wavefronts. Their wavelengths ranged from 4.0 km at the leading edge of the packets to 1.6 km at the trailing edge. They appear to be solitary wave packets excited by tidal flows over the shelf region.[10]

Danielle

Figure 3a shows the SAR swath across Danielle, and Fig. 3b shows the 85-GHz polarization corrected temperature (PCT) calculated from a SSM/I pass that occurred 30 min later. The 85-GHz channel has a 15-km resolution. The SAR image reveals five main features of interest:

1. The structure of the eye (A) and possible mesoscale features within
2. The principal rain band signature (E–E′)
3. Streaks on the surface between rain bands (B, C, and D)
4. Thunderstorm outflow structures in the outer convective band (F and G)
5. Evidence of graupel (granular snow pellets and soft hail) and ice signatures in the very bright returns from convective clouds (F, G, H, and I)

The outer principal rain band (E–E′) appears in the SAR image as a dark, curved feature with a jagged inner edge. From the adjacent

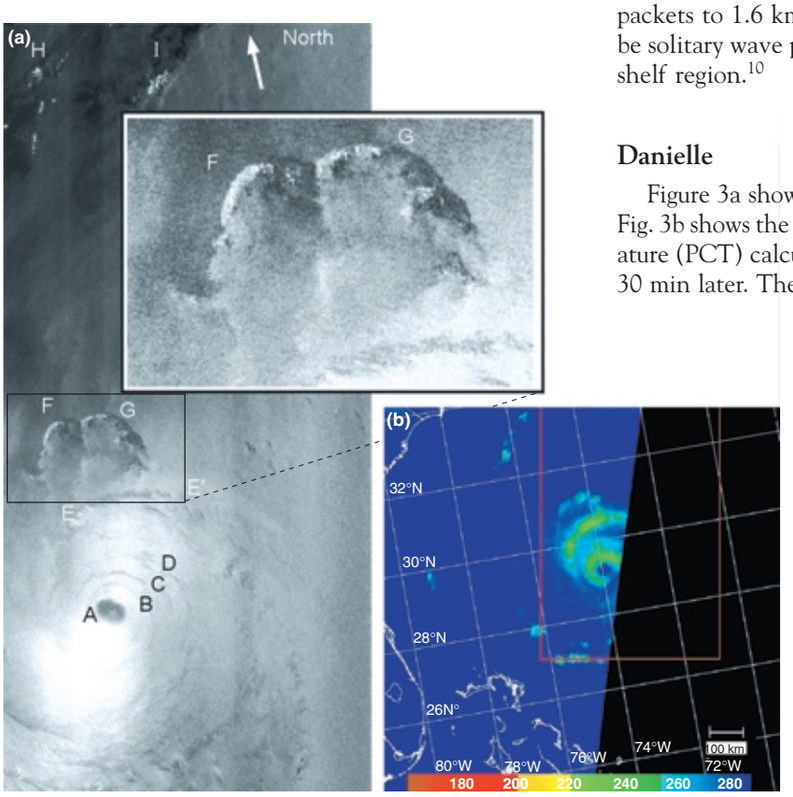

Figure 3. Radarsat SAR and SSM/I images from Hurricane Danielle on 31 August 1998. (a) SAR image at 1048 UT (430 × 900 km) (© Canadian Space Agency, 1998), and (b) SSM/I image at 1126 UT (1000 × 1000 km) with the same orientation as the SAR image. The red box outlines the SAR swath. Note that the SAR image extends farther north than the SSM/I image. The color bar indicates polarization-corrected brightness temperatures (K).

SSM/I image, it is seen that this feature is located along the inner edge of the main precipitation feature shown by the enhanced PCT values of the SSM/I. Although the scales are different in these two images, the edge of the region of precipitating cloud, identified by SSM/I, can be seen to coincide with the SAR feature. In the full-resolution image (Fig. 4) of this section of the SAR swath, the streak features have a circular orientation centered on the eye and converging toward the rain band. These features contribute to the ragged appearance of the inner edge of the dark band. This behavior suggests that enhanced inflow associated with roll vortices is directed toward the band and could be contributing to the intense convection by increasing the advection of heat and moisture.

The SAR image at F and G in Fig. 3a shows two curved features, like paw prints, that appear to be the leading edge of the gust fronts. The easternmost of these shows a sharp leading edge in which there is reduced radar return compared with the elevated brightness values associated with the ambient easterly wind around Danielle. It appears that the eastward-flowing gust-front air canceled the westward-flowing mean storm circulation, resulting in near-calm conditions behind this portion of the gust front.

This F–G region is far enough from the storm center that the mean wind speed is only about 5 m/s (as inferred from an HRD-generated wind field obtained from flight data collected between 2 and 5 h after the Radarsat image). The storm did not change dramatically during this time, so the general structure can be assumed constant. Surface radar features due to this type of mesoscale convective system were observed with ERS-1 in SAR image mode over the Gulf Stream off Florida, without the presence of a hurricane, and were discussed in detail by Atlas and Black.[7]

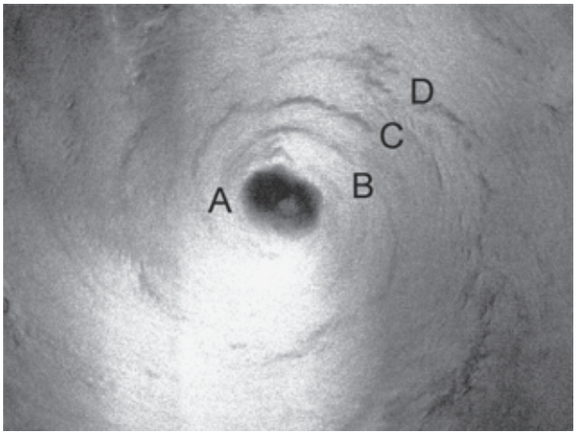

Figure 4. A 256 × 192 km portion of the Hurricane Danielle SAR image showing the eyewall region. A is the center, and B, C, and D indicate rain bands (© Canadian Space Agency, 1998).

The new features we observe in these outlying cells of Danielle are the small white spots within the rain cell (Fig. 3a, F–G region). The very bright spots are of the order of 800 m in diameter. They appear to be associated with thunderstorms forced by the extra uplift where the gust front meets the ambient air at the outer edge of these cells. Such storms are known to produce graupel (and possibly hail). That these bright spots could be due to ice in the rain clouds is verified by the 85-GHz polarization difference (or PCT) measured by SSM/I within 30 min of the Radarsat image. Depolarization of the 85-GHz emission from the sea is caused by randomly oriented ice particles in the cloud as the signal passes through this rain cell (Fig. 3b). The strongest depolarization is seen to occur in the region where the SAR image shows the bright spots (Fig. 3a).

The general pattern of F and G indicates two intersecting gust fronts that probably originated from intense super cell convection within the outer principal band to the south as much as an hour or so earlier. This signature is suggestive of severe weather within the principal rain band of Danielle at some earlier time, a diagnosis made possible through the joint use of SAR and SSM/I images.

The eyewall region of Danielle shown in a portion of the SAR image (Fig. 4) has an oval-shaped appearance with a thin band of very bright return along the northern semicircle, inside of which the brightness falls off abruptly. In the southern semicircle, the drop-off of bright return inside the eye is not as abrupt, but an enhanced brightness tongue appears to protrude from the south eyewall into the center (A). In other storms, such as Hurricane Luis in 1995,[11] this type of intrusion, whether associated with a wind enhancement, as we suspect, or enhanced ice in the upper levels associated with banding, is associated with the formation of an eyewall mesovortex and a strong eyewall asymmetry. This enlarged image also provides fine-scale detail of rain bands at points B, C, and D of Fig. 3, and reveals the presence of rolls with spacing similar to those noted in Bonnie.

Georges

The image from the SAR pass over Georges (Fig. 5a), shown with Key West NEXRAD reflectivities (Fig. 5b), covered the eastern semicircle of the storm. The western boundary of the SAR image coincides with the second rain band outward from the eyewall (A–A′), about 90 km east of the center. The image sampled a convectively active third rain band from the center (B–B′) and a newly developing band (C–C′) 250 km east of the center and about 90 km from Key West. These rain bands show the same characteristic features described for Bonnie and Danielle.

In addition, the band B–B′ shows a sharp outer edge to the dark patches, with several broad swaths along the

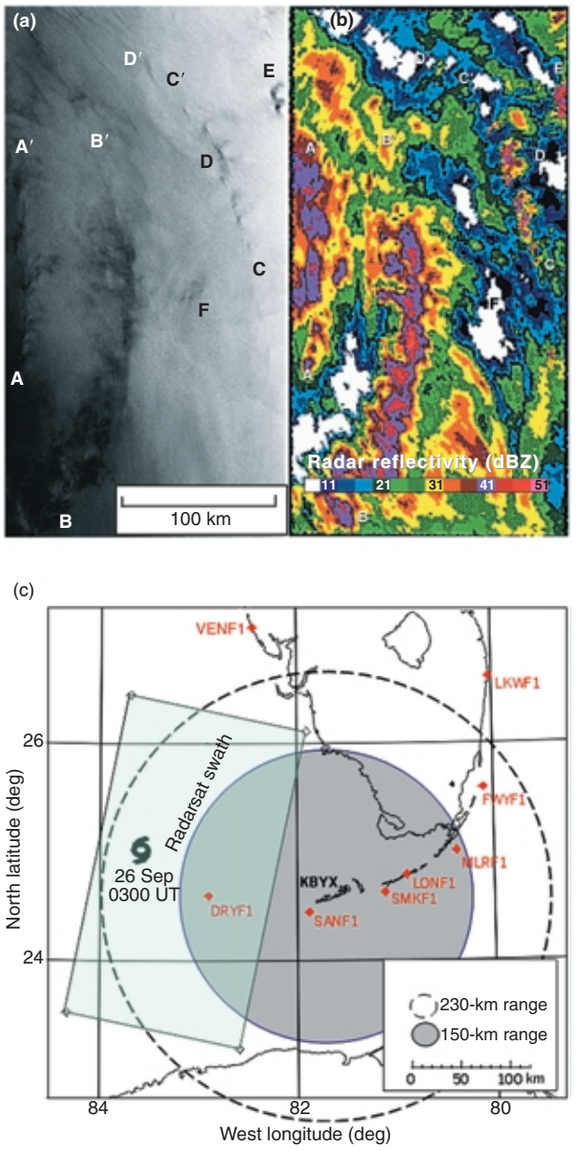

Figure 5. Radarsat SAR and WSR-88D images from Hurricane Georges on 26 September 1998. (a) 182 × 330 km SAR image at 1135 UT (© Canadian Space Agency, 1998), and (b) the portion of the lowest sweep of the Key West, Florida, WSR-88D radar (KBYX) at 1133 UT. Gray and color scaling are as in Fig. 1. The WSR-88D image was rotated and scaled to match the SAR image. WSR-88D data were supplied by the National Climatic Data Center, Asheville, North Carolina. (c) Map showing SAR swath location relative to KBYX and C-MAN surface stations. Shaded area indicates WSR-88D Doppler coverage. The rectangle designates the area shown in (a).

band extending inward. These swaths correspond to similar features in the NEXRAD radar image. They appear to represent inward-tilting convective elements that spread stratiform precipitation inward across the band. This is most likely caused by the presence of more inward-directed winds aloft in this quadrant due to a stronger, large-scale southeasterly flow aloft than at the surface. The source of the reduction in backscatter is again ambiguous. It could be due to either damping of the surface capillaries or attenuation by the rain in the intervening atmosphere.

Band C–C′ was clearly in the process of developing at the time of the SAR pass. Enhanced brightness can be seen just outward of the small black features, indicating intense convective rain on scales of the order of 1 km. A broad, bright region northwest of the three northern cells in this band ends in what appears to be an outflow boundary along D–D′. This phenomenon illustrates the many scales of motion occurring simultaneously in a tropical cyclone. Most likely, as this outflow boundary propagates from the new band C–C′ toward B–B′, it will be modified by energy fluxes from the sea and will contribute to the evolution of the storm.

The strongest convective cells are seen at E, where two dark features are observed with small, curved outflow boundaries just beginning to form to the west of the spots. Very bright returns are observed east of the dark spots, suggestive of ice and graupel in the interior of the clouds or enhanced surface inflow. Feature F is the island and reefs around Dry Tortugas.

Longitudinal roll features are also seen at the very top of the SAR image at a slight angle to the cyclonic wind direction. The NEXRAD image shows very weak or no rain in this region.

Mitch

The image from the SAR pass over Mitch is shown in Fig. 6a. Figure 6b shows the rain inferred from the TRMM satellite at a 5-km resolution. The TRMM overpass occurred 3.5 h before the Radarsat pass. The TRMM rain pattern illustrates the banded precipitation structure that appears in the SAR imprints. A first rain band 30 km east of the center is seen in the western edge of the image at A, and a stratiform rain band is seen along B–B′ about 40 to 60 km east of the center. A third, more convective band, C–C′, occurs about 70 to 120 km northeast of the center. Swan Island (Islas Santanilla) is located at D. Strongly convective outer bands are noted along E–E′.

At 150 to 180 km from these bands (E), dark features are seen to spread to the northeast, much the same as ice on the upper portion of a cloud would spread as it reached the outflow layer. Since Radarsat is a C-band radar, it would take a substantial amount of ice and large particles to have this strong an effect due to absorption. C-band radars are used for their ability to penetrate clouds with little absorption. However, a hurricane of Mitch's intensity appears to defy that general advantage. We speculate that these dark regions could be caused by rain on the surface that is

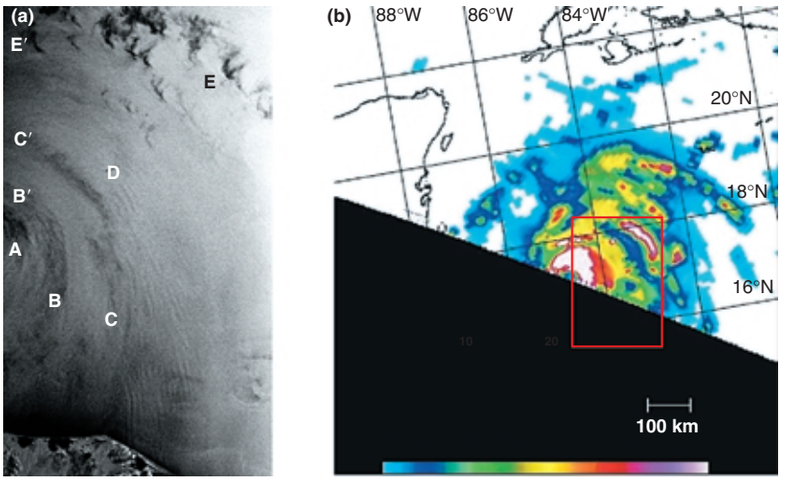

Figure 6. Radarsat SAR and TRMM images from Hurricane Mitch on 27 October 1998. The SAR image (a) at 1133 UT covers 184 × 322 km. The TRMM image (b) at 0837 UT has the same orientation as the SAR image and is 1060 × 1100 km. The red box outlines the SAR swath. The color scale is TRMM rainfall in mm/h. Green = 10 mm/h, red = 20 mm/h.

related to the upper clouds, if the lower clouds are nucleated by ice falling from the upper stratiform cloud (so-called "seeding").

Figure 6a shows a multitude of the band features for Mitch that were seen in Bonnie. Here, they cover the whole region between two major rain bands (B–B′ and C–C′), reaching all the way to the coast of Honduras at the bottom of the image and, possibly, across it. This does not prove that roll vortices do not exist inside the rain bands, but only that no SAR signature has resulted. However, the convective updrafts in the intense rain areas disturb the boundary-layer top and would, therefore, make the rolls unlikely there. The rain image from TRMM (Fig. 6b) produced from the radar and microwave radiometer data shows the location of the rain bands and identifies the region occupied by the large-scale rolls as the region between rain bands.

CONCLUSIONS

Radarsat SAR images in the ScanSAR wide mode can contribute exceptional details about the structure and distribution of rain cells and rain bands in a hurricane when the storm is still too far from the coastline to be observable by coastal radars. We cannot yet determine from the available data whether the reduced backscatter under rain regions is due to surface roughness changes or attenuation in the atmospheric path by the rain. The bright features seen in the convective complex of Danielle illustrate that the intense regions capable of producing ice particles are very narrow and seem to be absent in most of the convective rain cells (although the resolution and sensitivity may not be sufficient for SAR to "see" them in all circumstances).

Similar signatures of ice within clouds were seen to the north of Danielle in an independent weather system, adding credence to our suggestion that the SAR sees considerable internal detail in the graupel and ice-generating region of clouds. This observation means that these patterns may at times be overlaid on surface wind patterns within the inner core of tropical cyclones, and that considerable effort is needed to learn to separate the signatures of the altered surface roughness and absorption emissions along the radar transmission path. Concurrent rain radar and microwave satellite data from SSM/I and TRMM will be useful, as will aircraft and *in situ* measurements.

The most exciting new discovery, seen in three of these Radarsat images, is the recognition of secondary circulations in the atmospheric boundary layer (roll vortices) in the region between the main rain bands of a hurricane. They are aligned with the surface wind within 20°, as expected (we know the wind direction in hurricanes to good accuracy from the cloud structure). The rolls' wavelengths of 4 to 6 km indicate a boundary layer of 2 to 3 km.[12] That height is of the order of typical trade wind boundary layers[13] and much higher than the boundary-layer depth of the region of inflow into the rain bands, which is of the order of 500 m.

The observations of Wurman and Winslow[14] have shown prominent wind streaks with a scale of approximately 600 m in the inner core, about the scale of the boundary-layer depth as defined by the layer of constant potential temperature. The radar observations have suggested a boundary-layer scale of variability of 3 to 6 km, several times the depth of the boundary layer between the outer bands. Gall et al.[15] analyzed National Weather Service radar collected in hurricanes Hugo, Andrew, and Erin by correlating echoes from successive scans and found similar structures, although they speculate that the features may extend 5 to 6 km up in the atmosphere, deeper than boundary-layer rolls. This appears to be a new and prominent scale of variability in the tropical cyclone boundary layer.

The significance of this discovery for the structure and dynamics of the rain bands and the regions between them is not certain. However, the pervasiveness of these features in all of the storms, and particularly in the most intense one, Mitch, indicates that SAR imagery could contribute to research on the planetary boundary layer in hurricanes, which is very difficult to measure by other means. The information in the SAR

images could be assimilated into mesoscale numerical models, together with the rain radar and flight data, to produce a more complete description of a storm.

These results may also have profound implications for estimates of momentum and sensible and latent heat fluxes to and from the sea, respectively, in tropical cyclones, since roll vortices are known to enhance these fluxes by 10 to 20%. We suggest that roll vortex features be further documented by additional SAR data collected in future tropical cyclones coincident with low-level aircraft measurements of turbulence, vertical velocity, and Doppler radar, together with airborne scatterometer observations of the surface winds and scanning radar altimeter observations of the surface waves.

REFERENCES

[1]Vachon, P. W., and Olsen, R. B., "Radarsat: Which Mode Should I Use?" *Backscatter* **9**, 14–20 (1998).

[2]Vachon, P. W., Katsaros, K., Black, P., and Dodge, P., "Radarsat Synthetic Aperture Radar Measurements of Some 1998 Hurricanes," in *Proc. IEEE 1999 Int. Geoscience and Remote Sensing Symp. (IGARSS '99)*, Hamburg, Germany, pp. 1631–1633 (1999).

[3]Burpee, R. W., Franklin, J. L., Lord, S., Tuleya, R., and Aberson, S. D., "The Impact of Omega Dropwindsondes on Operational Hurricane Track Forecast Models," *Bull. Am. Meteorol. Soc.* **77**, 925–933 (1996).

[4]Powell, M. D., Houston, S. H., Amat, L. R., and Morisseau-Leroy, N., "The HRD Real-Time Hurricane Wind Analysis System," *J. Wind Eng. Indust. Dyn.* **77/78**, 53–64 (1998).

[5]Willoughby, H. E., Clos, J. A., and Shoreibah, M. G., "Concentric Eye Walls, Secondary Wind Maxima, and the Evolution of the Hurricane Vortex," *J. Atmos. Sci.* **39**, 395–411 (1982).

[6]Powell, M. D., "Boundary Layer Structure and Dynamics in Outer Hurricane Rain Bands. Part I: Mesoscale Rainfall and Kinematic Structure," *Mon. Wea. Rev.* **118**, 891–917 (1990).

[7]Atlas, D., and Black, P. G., "The Evolution of Convective Storms from Their Footprints on the Sea as Viewed by Synthetic Aperture Radar from Space," *Bull. Am. Meteorol. Soc.* **75**, 1183–1190 (1994).

[8]Thompson, T. W., Liu, W. T., and Weissman, D. E., "Synthetic Aperture Radar Observation of Ocean Roughness from Rolls in an Unstable Marine Boundary Layer," *Geophys. Res. Lett.* **10**, 1172–1175 (1983).

[9]Alpers, W., and Brümmer, B., "Atmospheric Boundary Layer Rolls Observed by the Synthetic Aperture Radar Aboard the ERS-1 Satellite," *J. Geophys. Res.* **99**, 12,613–12,621 (1994).

[10]Apel, J., "Observations of Oceanic Internal and Surface Waves for the Earth Resources Technology Satellite," *J. Geophys. Res.* **80**, 865–881 (1975).

[11]Hasler, A. F., Palaniappan, K., Kambhammetu, C., Black, P., Uhlhorn, E., and Chesters, D., "High-Resolution Wind Fields Within the Inner Core and Eye of a Mature Tropical Cyclone from GOES 1-Min Images," *Bull. Am. Met. Soc.* **79**, 2483–2496 (1998).

[12]Brown, R. A., "Seven-Day Flow Model for the Planetary Boundary Layer," *J. Atmos. Sci.* **27**, 742–757 (1970).

[13]LeMone, M. A., "The Structure and Dynamics of Horizontal Roll Vortices in the Planetary Boundary Layer," *J. Atmos. Sci.* **20**, 1077–1091 (1973).

[14]Wurman, J., and Winslow, J., "Intense Sub-Kilometer-Scale Boundary Layer Rolls Observed in Hurricane Fran," *Science* **280**, 555–557 (1998).

[15]Gall, R., Tuttle, J., and Hildebrand, P., "Small-Scale Spiral Bands Observed in Hurricanes Andrew, Hugo, and Erin," *Mon. Wea. Rev.* **126**, 1749–1766 (1998).

ACKNOWLEDGMENTS: Julie Cranton and John Wolfe (Canada Center for Remote Sensing) contributed to the acquisition and processing of the Radarsat data; the WSR-88D radar data for hurricanes Bonnie and Georges were collected by the Morehead City, North Carolina, and Key West, Florida, Weather Service Forecast Offices and were supplied by the National Climatic Data Center in Asheville, North Carolina. Supporting information from the SSM/I and TRMM was taken from the Web site of Jeffrey Hawkins and co-workers of the Naval Research Laboratory at http://www.nrl.navy.mil/index.htm. We thank Robert Beal of APL and William Pichel and Pablo Clemente-Colón of NESDIS for helpful discussions. We also thank Gail Derr for her able production of the manuscript.

THE AUTHORS

KRISTINA B. KATSAROS is with the Atlantic Oceanographic and Meteorological Laboratory, Miami, FL. Her e-mail address is katsaros@aoml.noaa.gov.

PARIS W. VACHON is with the Canada Center for Remote Sensing, Ottawa, Ontario. His e-mail address is paris.vachon@ccrs.nrcan.gc.ca.

PETER G. BLACK is with the Atlantic Oceanographic and Meteorological Laboratory, Miami, FL. His e-mail address is black@aoml.noaa.gov.

PETER P. DODGE is with the Atlantic Oceanographic and Meteorological Laboratory, Miami, FL. His e-mail address is dodge@aoml.noaa.gov.

ERIC W. UHLHORN is with the Atlantic Oceanographic and Meteorological Laboratory, Miami, FL. His e-mail address is uhlhorn@aoml.noaa.gov.